

## Dust Coulomb Balls: Three-Dimensional Plasma Crystals

Oliver Arp,\* Dietmar Block, and Alexander Piel

*IEAP, Christian-Albrechts-Universität, D-24098 Kiel, Germany*

André Melzer

*Institut für Physik, Ernst-Moritz-Arndt Universität, D-17489 Greifswald, Germany*

(Received 10 May 2004; published 15 October 2004)

First experimental investigations of spherical three-dimensional plasma crystals consisting of hundreds or thousands of micrometer-sized polymer particles suspended in a radio-frequency gas discharge are described. These “Coulomb balls” are not subject to the formation of dust-free regions (voids) and have an unusual structure of nested crystalline shells. While small systems are in a solid phase, large systems show melting effects.

DOI: 10.1103/PhysRevLett.93.165004

PACS numbers: 52.27.Lw, 52.27.Gr, 52.35.Fp, 82.70.Dd

Plasma is generally considered as the most disordered state of matter. Yet, micrometer size dust particles embedded in an electrical discharge can form regular patterns, the so-called plasma crystals [1–3] at room temperature. Usually, because of gravity, the heavy dust particles sediment to the bottom of the plasma, where they are levitated in the space-charge sheath above a horizontal electrode. There, flat nearly two-dimensional (2D) crystals are formed, which have been widely used to study phase transitions [4,5], fluid motion in strongly coupled systems [6], or a variety of wave phenomena [7]. Attempts to create homogeneous three-dimensional crystals in the plasma volume either under microgravity [8] or by thermophoretic levitation, i.e., a temperature gradient in the neutral gas that exerts a net upward force on the dust particles [9] were hampered by the appearance of dust-free regions (voids) [10] that result in hollow particle arrangements. Voids are attributed to the (ambipolar) outflow of ions from the plasma center, which exerts a drag force [11] on the dust particles that is stronger than the opposing electric field force.

Plasma crystals are examples of strongly coupled systems. Matter is said to be strongly coupled, when the interaction energy of neighboring particles is larger than the energy of a particle’s random motion. This is true for liquids and solids, where neutral atoms are densely packed. For particles with charge  $Ze$  interacting by Coulomb potentials, coupling is measured by the parameter

$$\Gamma = \frac{Z^2 e^2}{4\pi\epsilon_0 b kT}, \quad (1)$$

the potential energy at the nearest neighbor distance  $b$  in units of the thermal energy. The liquid-solid transition occurs when  $\Gamma > 170$ . Typical gaseous plasmas are weakly coupled, because they are hot and dilute. Strongly coupled plasmas are only found at high density and low temperature, e.g., in white or brown dwarf stars or in the interior of the giant planets. For the understand-

ing of these objects, the liquid and solid states of strongly coupled plasmas are a field of high interest.

The plasma crystal formed by dust particles floating in a thin layer above an electrode has already proven to be a convenient and powerful model system to study strong coupling effects in two dimensions [4–6]. Unfortunately, the strong electric fields in the vicinity of the electrode do not only levitate the dust but also cause a directed ion flow that again results in an anisotropic, aligned crystal ordering [12–14]. In some cases, bcc-like [15,16] or hcp and fcc [17] structures were reported in multilayer systems. However, those systems were still confined to the plasma boundary layer. Another example for a strongly coupled charged-particle system are trapped laser-cooled ions [18,19], which can also form large Coulomb crystals [20].

Plasma crystals are notably different from ion crystals. The dust particles are negatively charged by the surrounding plasma and carry thousands of elementary charges. Therefore, the regime of strong coupling is already reached at room temperature whereas ions crystallize only at millikelvin temperatures. Further, the Coulomb interaction of dust particles is shielded to a certain extent by the positive plasma ions. Finally, the comparatively large size of the dust particles allows direct observation by simple video microscopy and slows down dynamic processes to typical frequencies of a few Hertz, quite unlike strongly coupled colloidal suspensions [21], where particle motion is heavily damped. Therefore, this system is ideally suited for studying the thermodynamics and dynamics of strongly coupled matter with “atomic resolution.”

In the following we present the discovery of void-free “Coulomb balls,” i.e., spherical particle clouds, in which hundreds or thousands of identical plastic spheres are arranged in nested crystalline shells. This unusual structure was found earlier in magnetically confined ion crystals [22].

Plasma is produced in the capacitively coupled parallel plate discharge at 13.56 MHz described earlier [13]. The gas pressure (argon) is (50–150) Pa and the discharge

voltage (40–60)  $V_{pp}$ . The essential modifications for confining Coulomb balls are the following: The particles are levitated by thermophoretic forces, which is accomplished by heating the lower plate to (30–80) °C. The combination of higher pressure and lower rf-power usually gives better confinement. The direction of the ion drag force, which usually causes a void in the plasma center, is reversed by confining the dust cloud radially in a short upright glass tube with 40 mm by 40 mm cross section. In this way, the discharge is operated with a higher plasma density in the outer zone than inside the tube. We conjecture that, in this geometry, the dust cluster is confined by the ion drag force from inwards flowing ions. Such a steady flow is possible, because recombination of ions at the inner glass walls forms the necessary particle sink to terminate the inflow of ions. Surface charges on the glass wall may also contribute to the confinement.

Spherical monodisperse Melamine formaldehyde particles of 3.4  $\mu\text{m}$  diameter are used. The particles are illuminated with a vertical fan of laser light, which is moved together with a charge-coupled device camera to give a set of several hundred adjacent slices. The particle positions in each frame are determined with subpixel resolution while the depth information is taken from the maximum of the light intensity curve in subsequent frames.

Figures 1(a) and 1(b) show vertical sections through a Coulomb ball with five mm diameter consisting of 190 particles. The section touching the front side indicates the hexagonal order on the surface. Because of a small misalignment of the laser fan the first contact is not at the center but slightly shifted to the left. The central cut in Fig. 1(d) demonstrates the absence of voids. The side and top view of this Coulomb ball is shown in Figs. 1(c) and 1(d) in terms of projections of all particles into the  $x$ - $z$  respectively  $x$ - $y$  plane. The spherical shape, which becomes evident from the dotted circles in both projections, reflects the isotropic spherical confinement of the cluster. A further observation is the absence of the arrangement of the particles in vertical chains, which was reported for the sheath region (e.g., [13]) as a consequence of the formation of wakefields by streaming ions, or in an rf-discharge without compensation of gravity [14].

Figure 2 shows the analysis of the structure for the 190-particle cluster. According to molecular dynamics (MD) simulations [23–25], we expect Coulomb crystals to form distinct “onion shells,” in which the particles are evenly arranged in patterns with five or six neighbors. Such kind of shell structure becomes clearly visible when the particle positions are plotted in cylindrical coordinates  $\rho = (x^2 + y^2)^{1/2}$  and  $z$  [Fig. 2(a)]. The shells are clearly separated and spherical in the lower half of the Coulomb ball. In the upper half a certain number of defects with particles at intershell positions is found. This is a general tendency seen in most experiments. The ratio of the inter-

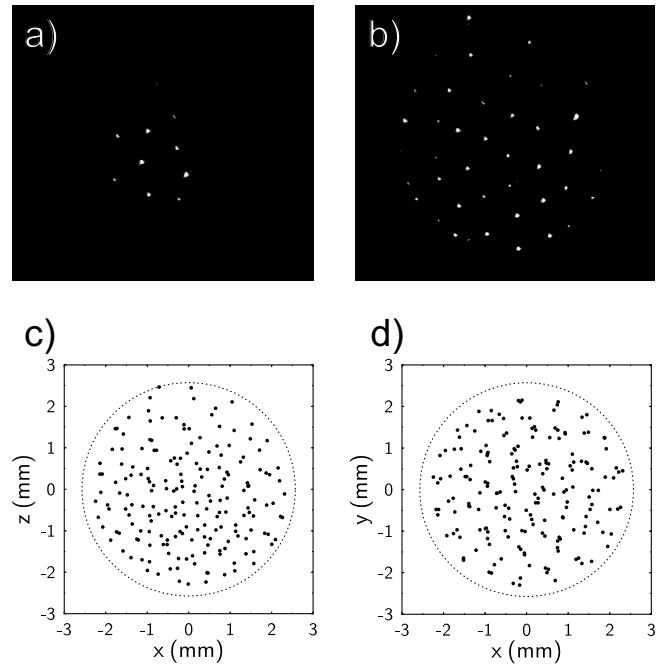


FIG. 1. (a) A vertical section touching the surface of a Coulomb ball with 190 particles shows a hexagonal particle arrangement. (b) The central section proves the absence of voids. (c) The projection of all particles into the vertical plane and (d) into the horizontal plane shows the spherical shape of the cluster.

shell distance (0.63 mm) to the interparticle distance (0.715 mm) is in close agreement with simulation results [23]. In the experiment we find four shells with occupation numbers 2, 21, 60, and 107. Hasse [23] gives the same number of shells for the neighboring 192-particle

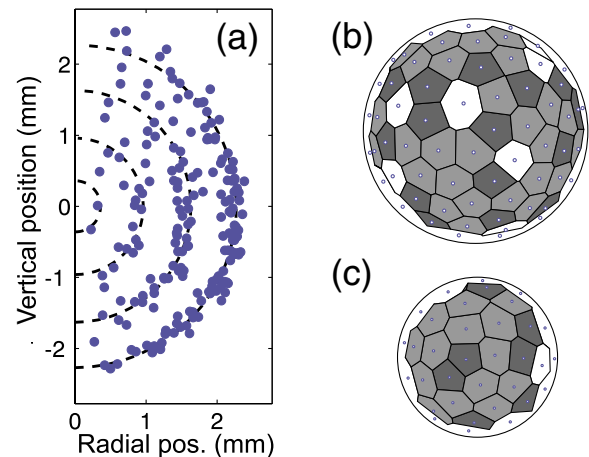


FIG. 2 (color online). The 190 particle cluster. (a) The shell structure becomes evident by projecting all particles into the  $(\rho, z)$ -plane irrespective of their angular position with regard to the  $z$  axis. (b) Bottom view of Coulomb ball showing the arrangement of the particles (small circles) in the shells  $M = 4$  and (c)  $M = 3$  superimposed by the Voronoi cell analysis. Hexagons are shaded light gray and pentagon dark gray.

Coulomb cluster, however, the occupation numbers 1, 18, 59, 114 are slightly different, which may be attributed to the observed particles at interstitial positions.

Figure 2(b) shows the outer shell ( $M = 4$ ) of the 190 particle cloud, where the particles are found evenly distributed. The number of neighbors for each particle is determined by a Voronoi analysis on the sphere. Besides the expected hexagons and pentagons, we find defect structures with seven neighbors. The inner  $M = 3$  shell [Fig. 2(c) has only hexagons and pentagons]. This kind of surface structure is expected because of the incompatibility of a pure hexagonal lattice with a curved surface and the incommensurability of particle numbers in adjacent shells.

The solid phase of this system can be substantiated from the following considerations. First, the shell structure is a feature of the typical order inside a cluster. Second, the motion of an individual particle is confined to a small region around the center of each Voronoi cell. The root-mean-square amplitude of the random motion is calculated in one  $x$ - $z$  section and corrected for the not observed  $y$  direction yielding less than 5% of the interparticle distance. This is smaller than the critical 10% value for melting according to the Lindemann criterion and indicates that the system is sufficiently far from the melting point. Third, we compare the coupling factor  $\Gamma$  with that of an infinite system [26]. The charge on the dust particles can be estimated from the electron temperature (e.g., [7]), yielding  $Z = 4700$  for  $3.4 \mu\text{m}$  particles for  $T_e = 2 \text{ eV}$ , resulting in a coupling factor of  $\Gamma = 1800$ . Even if we account for a reduction of  $\Gamma$  by a factor of 2 because of charge reduction in dense packing situations [27], it remains much larger than the melting point ( $\Gamma < 200$ ) of an infinite system. Schiffer [25] has performed simulations for the melting of 3D Coulomb clusters and found that the critical value of  $\Gamma$  depends on the system size. He found the empirical formula  $\Gamma^{-1} = \Gamma_0^{-1}(1 - 0.98F)$  (where  $\Gamma_0$  is the critical value for an infinite system and  $F$  the fraction of ions in the outer layer), which gives a critical  $\Gamma = 413$  for our 190-particle Coulomb cluster.

A medium size Coulomb ball with  $N = 2823$  particles and 12 mm diameter is shown in Fig. 3(a). The representation in cylindrical coordinates ( $\rho, z$ ) shows the formation of outer shells in terms of a clustering of points. Visual inspection of the center of the ball shows no pronounced shells. The shells become still clearer visible in the radial distribution [Fig. 3(b)]. The arrows mark the three outer shells. The pair correlation function in Fig. 3(c) counts the number of particles at a given interparticle distance. We have calculated the pair correlation function for the entire cluster (solid line) and for the central  $N/3 = 941$  particles (dotted line). For both curves there is a sharp peak of nearest neighbors and a second peak of next but one neighbors, but practically no particles are found closer than the nearest neighbor peak

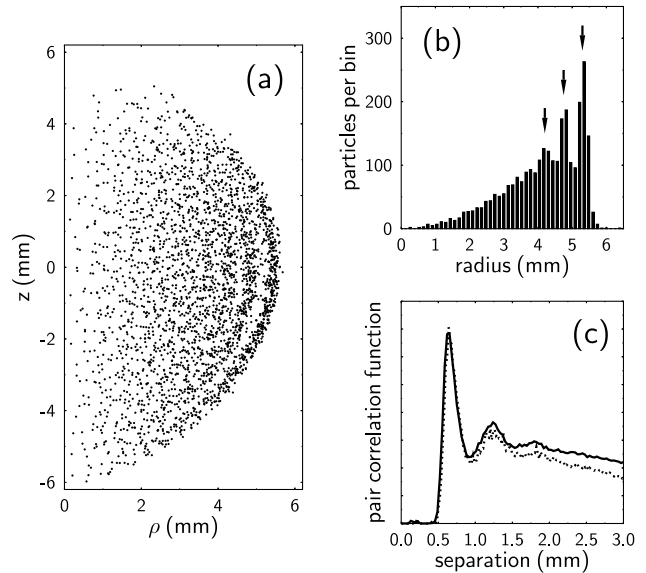


FIG. 3. (a) Structure of a medium size cluster with  $N = 2823$  particles in ( $\rho$ - $z$ ) coordinates. (b) Radial distribution of the particles showing three distinct outer shells (arrows). (c) Pair correlation function for the total cluster (solid line) and the central 941 particles (dotted).

(except for a very small number of artefacts around 0.2 mm separation from the particle identification algorithm). This structure is typically found in solids and liquids, where atoms are densely packed. In the present case, where the particles are more than a hundred times smaller than their separation, it is an indication of the strong coupling, i.e., the Coulomb repulsion is very much stronger than the counteracting thermal agitation.

The first and second maximum of the solid and dotted curve are practically located at the same position. The faster decay of the dotted line is due to missing correlations near the surface, which becomes more significant for small spheres. The positional order is therefore practically the same in the center as in the entire Coulomb ball. By visual inspection of the central part from many different orientations, we could not find any hint at bcc order. Bulk order with bcc structure was reported from much larger systems, such as ion crystals with  $10^5$ – $10^6$  ions in a Penning trap [20].

We conjecture that the outer layers are frozen under the influence of the pressure from the plasma trap while the center is in a liquid or glassy state with positional but no significant orientational order. Simple attempts to “anneal” the structure by gently shaking the Coulomb ball through an applied low-frequency sinusoidal voltage to the lower electrode were not successful.

At the highest particle numbers of our experiments, interesting new features are observed. Figure 4 shows a section through the center of a huge Coulomb ball with more than 6000 particles and a diameter of 15 mm. The ball is mostly spherical with some imperfections close to the top. Except for a certain separation of the outermost

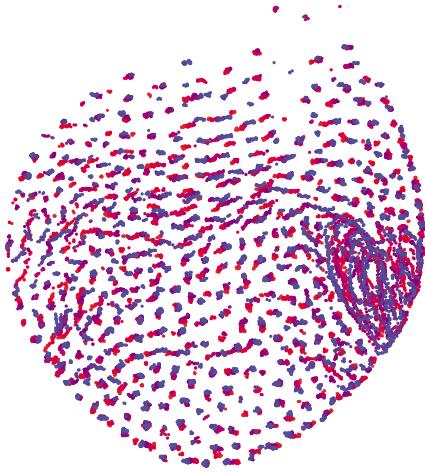


FIG. 4 (color online). Vertical section through the center of a huge Coulomb ball with  $N > 6000$  particles. The motion of all individual particles is traced by superimposing the particle positions in 1 s intervals for a total of 120 s. The system shows frozen domains as well as slow and fast fluid motion.

layer from the bulk there is no pronounced shell formation. In this Figure, each dot marks the position of a particle, which we have traced by superimposing a sequence of 120 consecutive still images taken at 1 s intervals. Even such huge Coulomb balls have a sufficiently high transparency that interior particles can be followed. The trajectories show that this Coulomb ball has regions with quite different dynamics. At the bottom, a solid region without noticeable particle motion is found. Further upwards, there are regions with slow motion (center) and fast motion (right-hand side). The alignment of neighboring trajectories and the low velocities (order of  $10 \mu\text{m s}^{-1}$ ) indicate that these regions are apparently in a liquid state. The finding of solid regions surrounded by flow regions resembles similar features of the melting process found in 2D crystals [4,5].

Summarizing, Coulomb balls are the long-sought-for spherical three-dimensional plasma crystals that are unaffected by the void phenomenon or chainlike order. We find close resemblance with the shell structure reported for laser-cooled ion crystals. This first survey of Coulomb balls of different size shows already a variety of interesting structural, dynamic and thermodynamic effects. We can imagine many directions of research with Coulomb balls, among them the dependence of phase transitions on system size, the formation of bcc order in the bulk of larger crystals, the role of fluctuations close to a phase transition, or the exploration of elastic properties by fundamental types of vibrations. In this way, Coulomb balls will certainly give important new insights into strongly coupled matter.

Part of this work was financially supported by DLR under Contract No. 50WM0039.

\*Electronic address: arp@physik.uni-kiel.de

- [1] J. H. Chu and L. I, *Physica* (Amsterdam) **205A**, 183 (1994).
- [2] H. Thomas, G. E. Morfill, V. Demmel, J. Goree, B. Feuerbacher, and D. Möhlmann, *Phys. Rev. Lett.* **73**, 652 (1994).
- [3] Y. Hayashi and K. Tachibana, *Jpn. J. Appl. Phys.* **33**, L804 (1994).
- [4] A. Melzer, A. Homann, and A. Piel, *Phys. Rev. E* **53**, 2757 (1996).
- [5] H. Thomas and G. E. Morfill, *Nature* (London) **379**, 806 (1996).
- [6] L. I, W.-T. Juan, C.-H. Chiang, and J. H. Chu, *Science* **272**, 1626 (1996).
- [7] A. Piel and A. Melzer, *Plasma Phys. Controlled Fusion* **44**, R1 (2002).
- [8] G. E. Morfill, H. M. Thomas, U. Konopka, H. Rothermel, M. Zuzic, A. Ivlev, and J. Goree, *Phys. Rev. Lett.* **83**, 1598 (1999).
- [9] H. Rothermel, T. Hagl, G. E. Morfill, M. H. Thoma, and H. M. Thomas, *Phys. Rev. Lett.* **89**, 175001 (2002).
- [10] J. Goree, G. E. Morfill, V. N. Tsytovich, and S. V. Vladimirov, *Phys. Rev. E* **59**, 7055 (1999).
- [11] M. D. Kilgore, J. E. Daugherty, R. K. Porteous, and D. B. Graves, *J. Appl. Phys.* **73**, 7195 (1993).
- [12] M. Nambu, S. V. Vladimirov, and P. K. Shukla, *Phys. Lett. A* **203**, 40 (1995).
- [13] A. Melzer, V. A. Schweigert, I. V. Schweigert, A. Homann, S. Peters, and A. Piel, *Phys. Rev. E* **54**, 46(R) (1996).
- [14] A. V. Zobnin, A. P. Nefedov, V. A. Sinel'shchikov, O. A. Sinkevich, A. D. Usachev, V. S. Filippov, and V. E. Fortov, *Plasma Phys. Rep.* **26**, 415 (2000).
- [15] J. Pieper, J. Goree, and R. Quinn, *J. Vac. Sci. Technol. A* **14**, 519 (1996).
- [16] Y. Hayashi, *Phys. Rev. Lett.* **83**, 4764 (1999).
- [17] M. Zuzic, A. V. Ivlev, J. Goree, G. E. Morfill, H. M. Thomas, H. Rothermel, U. Konopka, R. Sütterlin, and D. D. Goldbeck, *Phys. Rev. Lett.* **85**, 4064 (2000).
- [18] F. Diedrich, E. Peik, J. M. Chen, W. Quint, and H. Walther, *Phys. Rev. Lett.* **59**, 2931 (1987).
- [19] D. J. Wineland, J. C. Bergquist, W. M. Itano, J. J. Bollinger, and C. H. Manney, *Phys. Rev. Lett.* **59**, 2935 (1987).
- [20] W. M. Itano, J. J. Bollinger, J. N. Tan, B. Jelenković, and D. J. Wineland, *Science* **279**, 686 (1998).
- [21] H. Löwen, *Phys. Rep.* **237**, 249 (1994).
- [22] S. L. Gilbert, J. J. Bollinger, and D. J. Wineland, *Phys. Rev. Lett.* **60**, 2022 (1988).
- [23] R. W. Hasse, and V. V. Avilov, *Phys. Rev. A* **44**, 4506 (1991).
- [24] D. H. E. Dubin and T. M. O'Neill, *Rev. Mod. Phys.* **71**, 87 (1999).
- [25] J. P. Schiffer, *Phys. Rev. Lett.* **88**, 205003 (2002).
- [26] K. Kremer, M. O. Robbins, and G. S. Grest, *Phys. Rev. Lett.* **57**, 2694 (1986).
- [27] O. Havnes, G. E. Morfill, and C. K. Goertz, *J. Geophys. Res.* **89**, 10999 (1984).